Design and performance evaluation of a full turboelectric, distributed electric propulsion aircraft: preliminary results of EU project IMOTHEP

Eric Nguyen Van, Sebastien Defoort, David Donjat, Christophe Viguier, Marwan Ali, Toni Youssef, David Gerada, Christopher Gerada

DOI: 10.13009/EUCASS2022-6134

Design and performance evaluation of a full turboelectric distributed electric propulsion aircraft: Preliminary results of EU project IMOTHEP

Eric Nguyen Van, Sebastien Defoort*, Michael Ridel*, David Donjat* and Christophe Viguier**, Marwan Ali**, Toni Youssef** and, David Gerada***, Christopher Gerada***.*

**ONERA*

*** SAFRAN TECH*

**** University of Nottingham*

Eric.nguyen_van@onera.fr, Christophe.viguier2@safrangroup.com, D.Gerada@nottingham.ac.uk

Abstract

The IMOTHEP project aims at improving the performance prediction of Hybrid Electric Propulsion systems. This paper focuses on the Small and Medium Range (SMR) transport aircraft in a so-called 'conservative' (CON) configuration. The SMR-CON aircraft is a tube and wing aircraft featuring a full turboelectric distributed propulsion. The propulsive architecture and the sizing strategy of the propulsive components are presented as well as the Overall Aircraft Design tool used to size the aircraft and calculate the flight performances. The SMR-CON performances, taken at the end of the initial design loop, are evaluated by comparison with a reference entry into service 2035 aircraft and the main directions of research are given through sensitivity studies.

1. Introduction

1.1 Scope of the study : the IMOTHEP project

This paper presents intermediate results obtained in the scope of the European project « Investigation and Maturation of Technologies for Hybrid Electric Propulsion » or IMOTHEP. The main objective of the IMOTHEP project is to significantly improve the estimation of the potential offered by hybrid electric propulsion in order to reduce the fuel consumption and CO2 emissions of civilian transport aircraft. Four hybrid aircraft configurations are studied and compared to a reference turbofan aircraft representative of actual technology levels and a baseline aircraft representative of technology levels for Entry Into Service (EIS) 2035.

The four configurations are split into two segments: (i) regional transport aviation (REG) and (ii) Small to Medium Range (SMR) transport aircraft. Within each segment, a conservative and a radical aircraft configuration are studied. The conservative configuration is named after its proximity with conventional aircraft while the radical configuration explores more disruptive propulsion integration and aircraft layout.

This project gathers 27 European partners, and Canadian research institute. Each partner brings an expertise in some of the many disciplines, from components modelling to overall aircraft evaluation, which are needed to model and analyse a hybrid electric propulsion aircraft. The work is organised in three design loops:

- L0 : first conceptual design loop, independent or loosely coupled multi-disciplinary evaluation from Top Level Requirements.
- L1 : first multi-disciplinary design loop integrating models provided by different work-packages, especially models of hybrid electric components (electric motor, cables, converters, turboshaft, generator,…).
- L2 : second multi-disciplinary design loop integrating refined and higher fidelity models, and addressing transient effects.

This paper reports the overall aircraft performances of the SMR conservative (SMR-CON) aircraft taken at the end of L0 design loop. The SMR-CON aircraft explores the concept of a turboelectric distributed propulsion associated to a traditional tube and wing layout, hence the denomination 'conservative'. The motivation behind the concept are introduced in details in the next section.

DOI: 10.13009/EUCASS2022-6134

1.2 Motivations and key aspects of the distributed turboelectric architecture

Ultra High By Pass Ratio (UHBR) turbofan are viewed as the next major propulsion evolution to increase the fuel efficiency of civil transport aircraft [1]. However, with the actual strategy of incrementally improving a well known aircraft such as the A320 or B737, the integration of UHBR turbofans of large diameter under the wing is increasingly difficult due to geometrical, weight distribution constraints and handling quality concerns [2].

In IMOTHEP, the SMR-CON aircraft relies on the DRAGON concept which idea is to integrate large by-pass ratio in the form of distributed small electric fans. This is rendered possible by the efficiency of electric motors, which is independent of the size, contrary to turbomachines cores.

Figure 1: Rendering of the Dragon concept, the baseline for the SMR-CON aircraft.

The SMR-CON uses the traditional tube&wing layout with rear-mounted gaz turbine generator producing the electrical power. The power is then transmitted to the electric fans located at the trailing edge in the pressure side of the wing (see Figure 1). The increased surface area of the fans allows capturing more air and therefore increasing the by-pass ratio to well beyond what would be achievable with an UHBR engine.
The propulsive efficiency is considerably increased, however it comes at the cost of losses in the electrical power transmission and added weight. The integration of the electric fans under the wing, while still targeting a transonic cruise speed of Mach 0.78, also comes at a price in integration drag and added wetted surface area.

The concept was evaluated with an Overall Aircraft Design (OAD) tool in previous studies in [1] and [2] and despite the cost of installation of a hybrid electric propulsion chain, a better fuel efficiency was achieved with reasonable technology assumptions. These technology assumptions represent the weak point of the analysis, as it asks for a projection to EIS 2035. This requires the gathering and work of disciplinary specialist to give an estimation of achievable technology levels. This was partly done in the previous studies at a coarse level and re-enforcing this aspect was identified as future work, this was the context in which the IMOTHEP project started.

To improve the estimation of the potential of hybrid electric propulsion to improve fuel efficiency, the large consortium gathers disciplinary specialists tasked with improving the expected technology projection in their respective field. The preliminary work realised for the Dragon concept furnishes a baseline design for all partners to quick start the work and an OAD environment readily available to evaluate the disciplinary solutions at the aircraft level. Compared to the Dragon concept, the SMR-CON will beneficiate from inputs of disciplinary specialists taking care of electric power unit (electric motor and associated power electronic), turbomachine and thermal management system design.

The paper presents the status of the SMR-CON configuration at the end of Design Loop 0. At this point, a first survey of disciplinary solutions was completed and the feedbacks were used to evaluate the version 0 of the SMR-CON aircraft with the Top Level Requirements (TLARs) formulated by the consortium. Section 2 presents the OAD design tool and reference aircraft performances data. Section 3 describes the sizing procedure of the turboelectric propulsion chain of the SMR-CON. Section 4 presents the current performances of the SMR-CON aircraft and a comparison with the reference aircraft. Finally, the work initiated in the next design loop on electric propulsion unit design is introduced in part 5.

DOI: 10.13009/EUCASS2022-6134

2. Tool presentation and reference results

2.1 Mystic overall aircraft design software

Integrated OAD activities have been running at ONERA for a long time, but the existing tool suites were either based on commercial integration software, or not sufficiently modular to perform MDO studies. Therefore, in the recent years, and taking benefit of on-going internal studies on MDO, a large effort was undertaken to define a new, modular, flexible tool to conduct the configuration studies, first at L0 level.
A first, simplified version of the tool called FAST (Future Aircraft Sizing Tool) was initiated and shared with ISAE. The description can be found in [4], and its evolution towards an Open source version called FAST-OAD is described in [5]. An enhanced version, calibrated and improved with ONERA internal knowledge, has then been developed under the name of MYSTIC (see [6]), and was used in this study.

MYSTIC design logic was modified to accommodate the specificity of the hybrid electric architecture and notably the sizing of the different components of the propulsion chain. The design logic is explained and detailed in [3], and is summarized here for a better understanding:

1. Initiator. This block initializes the problem and finds a first estimate of the aircraft parameters.

Do

2. Initialize the MDA loop.
3. Size the components of the DEP chain, based on power levels from previous iteration.
4. Size the wing, in order to satisfy the criterion of *CL*max in approach configuration.
5. Compute an initial geometry, based on a few set of entries per component (such as aspect ratio, sweep or taper ratio).
6. Resize the geometry, iteratively changing the wing and landing gear position and the tails, in order to satisfy stability criterion on static margin.
7. Compute the trimmed polars at low and high speed, considering the geometrical output of step 5.
8. Compute the detailed mass breakdown, based on an upgraded version of the French norm 2001/D [7] to take into account mass of hybrid propulsion system.
9. Compute the trajectory of aircraft on a given design mission, using the data from step 6 and 7. The aircraft is modelled as a mass-point, and the time step approach is used for each mission leg.
10. Check the convergence. The driven parameter for the convergence is the operating weight empty OWE, which is estimated at step 7 (bottom-up approach through Mass breakdown assessment) and step 8 (top-down approach from Performance assessment): at convergence, these two values must match. In practice, it is required that the relative difference between the two is below 0.05%; if not, update the MTOW and proceed to next iteration.
11. Update the values for the next iteration

until 11 – 2 has converged.

12. Once that the aircraft is sized, this analysis can compute its performances over a typical operation range different from the design range.

2.2 IMOTHEP TLARs and reference aircraft performances

The Top Level Requirements agreed on for the IMOTHEP project are summarized in Table 1. In essence, they are close to the Ceras requirements except for the design payload increased at 106kg/pax or 15 900kg.

Table 1: Top Level Requirements considered in the IMOTHEP project

Parameter	Value
Range	2750 NM
Design payload	15900 kg (150pax @ 106kg/pax)
Cruise Mach number	0.78
Wing span limit	36 m
TOFL (ISA +15, sea level)	< 2200 m

DOI: 10.13009/EUCASS2022-6134

In order to obtain at a baseline aircraft for EIS 2035 to which the SMR-CON is compared, the following methodology is employed:

- Ceras design: The MYSTIC tool is first calibrated on the Ceras aircraft.
- REFX design: The technology level of 2014 and the A320NEO is reproduced essentially by adjusting the specific fuel consumption and the engine mass.
- REF design: The IMOTHEP TLARs are applied with EIS 2014 technology levels.
- BAS design : EIS 2035 technology levels (see Table 3) are considered (aircraft presented in section 4.2).

The Ceras, REFX and REF aircraft designs key parameters and performances metrics as obtained with MYSTIC are presented in *Table 2*. The Ceras benchmark shows the only significant difference is the lift to drag ratio, however since the cruise altitude is fixed at 35kft, the effective lift to drag ratio achieved in cruise are similar as the fuel burn are comparable. The REFX design shows the fuel efficiency improvement of 9% gained thanks to a high bypass ratio turbofan. Subsequently, the REF design is becoming heavier and consumes an additional 3.8% fuel compared to the REFX design.

Table 2: calibration and reference aircraft as calculated by MYSTIC

	Ceras data	MYSTIC		
	(2750 NM)	Ceras	A320neo REFX	A320neo REF
TOW (Kg)	74102	74953	74340	78266
OWE (Kg)	42100	42267	43422	44477
Propulsion weight (Kg)	7751	7729	8653	8672,5
Max L/D	17,43	16,06	16,22	16,45
Span (m)	34,07	34,04	34,4	35,3
Wing area (m^2)	122,4	123,4	124,9	131,4
Fuel burn (Kg)	15420	15472	14080	14620

3. Distributed turboelectric architecture

Previous work initiated the reflexion to provide high level of safety with distributed propulsion [8]. The Hybrid Distributed Electric Propulsion (HDEP) architecture of the SMR-CON, illustrated in Figure 2, was built on the outcome of this previous exercise. Although the number of components is subject to change, the interconnection methodology and the distribution of the components answer the same goals:

- To provide a cross-redundant electrical power distribution,
- To be robust to single component failure,
- To limit the oversizing of components.

The architecture features two turboshafts each mechanically coupled to two generators (GL and GR in Figure 2). Each generator is feeding two cores (Propulsion Bus DC + Fault Current Limiter + Breakers) in a cross-redundant DC connexion. As such, if one generator or one turboshaft fails, all cores can be powered by the remaining turbomachine/generators. Finally, each core distributes power to a cluster of electric fans symmetrically arranged on the wings so that the loss of one core, translating in a loss of thrust, does not produce parasitic yawing moment.

DOI: 10.13009/EUCASS2022-6134

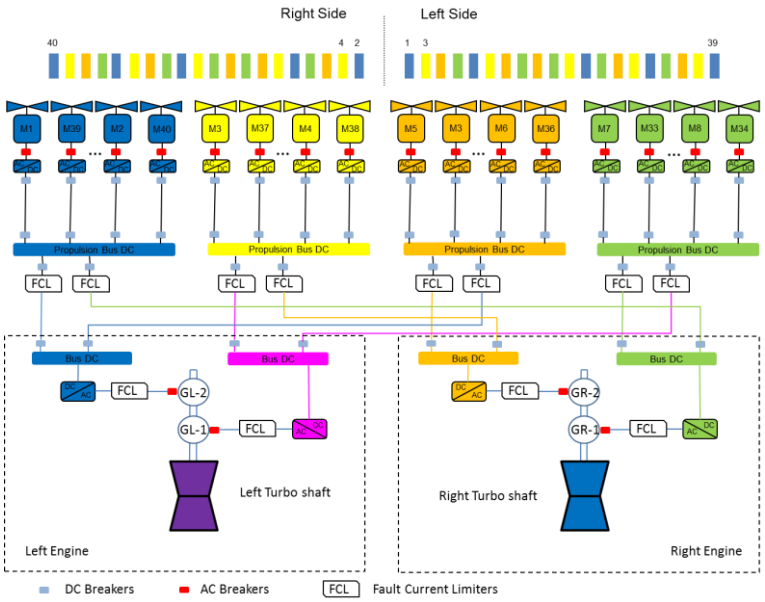

Figure 2: Turboelectric distributed architecture of the SMR-CON aircraft.

3.1 Sizing procedure of the propulsion chain

The sizing of the propulsion chain components is based on the assessment of relevant flight points including failure cases: One Core Inoperative (OCI), One Turboshaft Inoperative (OTI) and One Generator Inoperative (OGI). For these emergency conditions, a derivation of the CS-25 criteria is adopted: if there are 2 components (eg. Turboshafts), a climb gradient of 2,4% must be maintained with one failure. If there are 3 or more components (eg. Cores, Generators), a climb gradient of 3,0% must be maintained with one failure. This ensures that the remaining components are powerful enough to maintain flight safety in presence of one component failure.

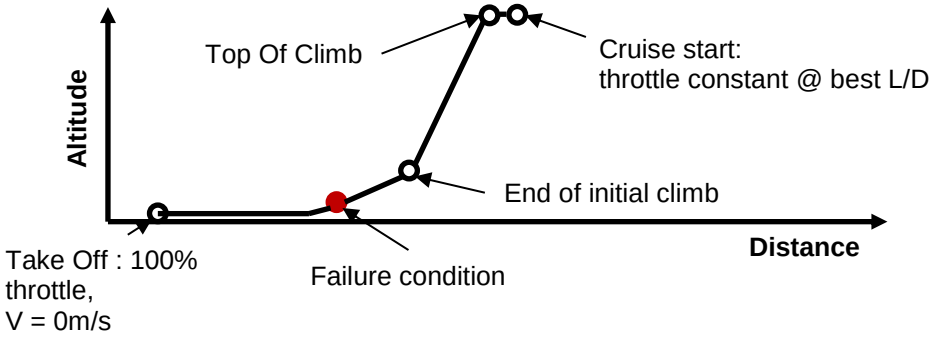

Figure 3: Flight points selected for the HDEP components sizing.

In addition to failure conditions, the following points of the nominal mission are considered relevant for the sizing (see Figure 3):

- Take off: size components to meet Take-Off Field Length requirement.
- End of initial climb: size components to meet climbing time requirement.
- Top Of Climb (TOC): size components to meet the objective residual vertical speed of 500ft per min.
- Beginning of cruise: the sizing condition for the efans to meet the objective cruise Fan Pressure Ratio (FPR).

For all sizing points, including the failure conditions, the thrust is calculated to meet the corresponding objective (effectively translated as climb gradient or determined with semi-empirical formula). The power demand of each HDEP components is then deduced from their efficiency and the number of operational element. Each component is sized for the maximum power demand over the list of sizing point.

DOI: 10.13009/EUCASS2022-6134

Only the fans are sized using a low fidelity thermodynamic model of a single stage compressor and nozzle, to achieve the targeted Fan Pressure Ratio (FPR) at the beginning of the cruise (typically 1.15 to 1.25). The geometry is then held constant and the fan model is used to determine the shaft power demanded to the electric motor for the rest of the flight conditions.

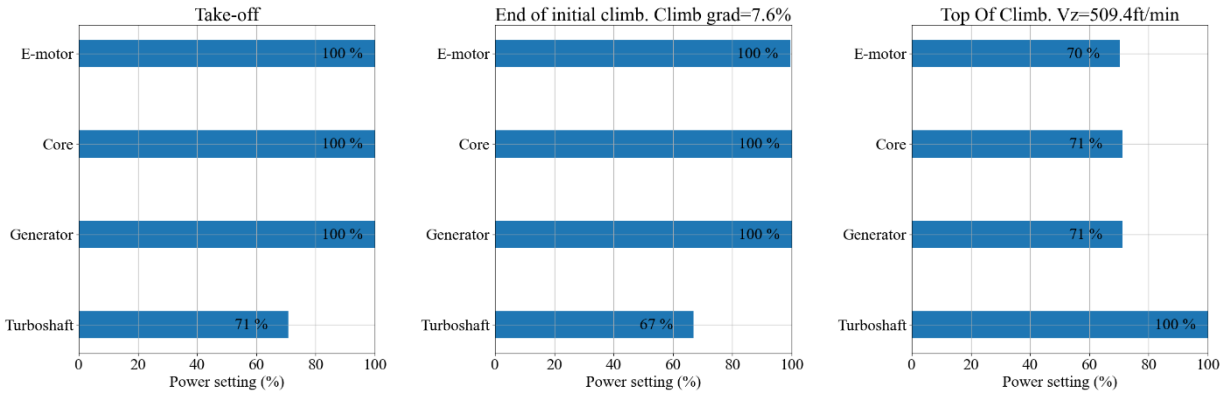

Figure 4: Power setting of main propulsive components during nominal mission condition (Left : Take-off. Middle : End of initial climb. Right: Top Of Climb)

Given the IMOTHEP TLARs, the most restrictive requirement to size the components was found to be the take off-field length for all components except the turboshafts that are sized for TOC conditions. The components rated power is then sufficient to ensure minimum flight performances in emergency situations. It should be stressed that 100% of the turbomachine power available at sea level is never used to perform the mission and the components are not sized to absorb that amount of power.

This is illustrated in Figure 4 and Figure 5 where the power setting of the main components for key flight points is shown for nominal flight conditions and emergency conditions.

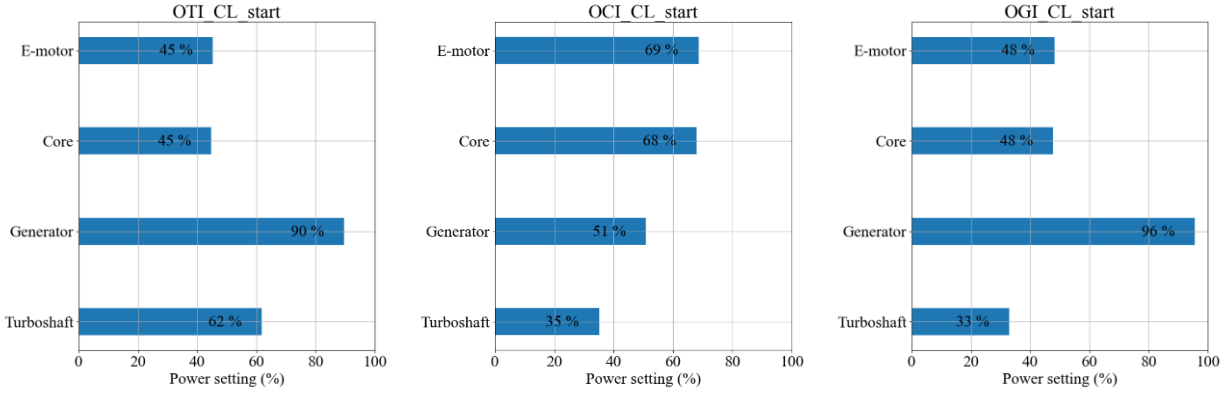

Figure 5: Power settings of the main propulsive components during failure scenario (Left: One Turboshaft Inoperative. Middle: One Core Inoperative. Right: One generator inoperative)

4.0 Concept performances and sensitivities

4.1 L0 technology assumption for 2035

Technology assumptions for EIS 2035 both for the BAS and the SMR-CON aircraft are shown in Table 3. The assumptions were provided by disciplinary specialists and agreed on by the project consortium. For the BAS aircraft they consist in an improvement in TSFC with respect to the NEO level and diverse aerodynamic and weight improvements. In comparison, the SMR-CON receives equivalent thermal efficiency improvement which translates as a PSFC at cruise condition of 145g/kWH (considering no offtakes and zero thrust generation).

Some aerodynamics and weight improvement of the BAS aircraft are not directly applied to the SMR-CON such as the contribution of morphing wing and lighter wing structure. In addition, it must be stressed that the SMR-

DOI: 10.13009/EUCASS2022-6134

CON uses an additional 5% drag penalty. All these differences are present to account for DEP integration penalty. On the contrary, it is expected that the SMR-CON could use a smaller landing gear, hence the beneficial weight improvement factor.

Note that a detailed integration of a UHBR turbofan was not performed. At this stage, the penalty is limited to weight and added wetted area which may produce optimistic results for the BAS aircraft.

Table 3: Technology level considered for EIS 2035 for BAS and SMR-CON aircraft

		EIS 2035 BAS Aircraft	**EIS 2035 SMR-CON**
Propulsion	SFC	-8.5% wrt NEO model	Equivalent thermal efficiency improvement
	Mass	+3.7% wrt NEO	Computed
	Wetted Area	Computed as a function of BPR = 16	Computed after ducted fan sizing
Aerodynamics	Morphing wing	3.3% on L/D	Not applicable
	Turbulent coating	-5% on CD0 wing	-5% on CD0 wing
	Winglet design	-10% on CD induced	-10% on CD induced
Component weight	Wing	-10%	-5%
	Fuselage	-5%	-5%
	Landing gear	-15%	-20%
	Pylons	-5%	-5%
	Seats	-25%	-25%

4.2 SMR-CON performances

The performances and key parameters of the SMR-CON are compared to the BAS and the REF aircraft in Table 4. The SMR-CON has a slightly higher OWE (+5.3%) explained mainly by the higher propulsion weight (+2.8T). However, thanks to some weight savings in the landing gear and the better fuel consumption, the MTOW is only 1% higher than the BAS aircraft. The SMR-CON span was increased to the maximum of 36m to improve the lift to drag ratio despite the penalty brought by the DEP. On the contrary the BAS still has a small wing and could have improved aerodynamics. In the end, the fuel burn is 6.5% better for the SMR-CON compared to the BAS and up to 26% improvement compared to the REF aircraft on the design mission of 2750NM.

Table 4: Key parameters and performance metrics for the SMR-CON compared to BAS and REF aircraft

	A320neo REF	**A320 2035 BAS**	**SMR-CON**
MTOW (kg)	78266	70882	71569
OWE (kg)	44477	40677	42824
OWE wrt REF	-	-8.5%	-3.7%
OWE wrt BAS	+9.3%	-	+5.3%
Propulsion weight (kg)	8672,5	8247	11082
Max L/D	16,45	17,68	17,35
Span (m)	35,3	34,3	36
Wing area (m²)	131,4	124,4	126
Fuel burn (kg)	14620	11571	10824
Fuel burn wrt REF	-	-20.9%	-26%

DOI: 10.13009/EUCASS2022-6134

Fuel burn wrt BAS	+26.4%	-	-6.5%
Reserve Fuel (kg)	3250	2636	1920
TOFL (m)	1866	1957	1946

The HDEP components characteristics used to calculate the SMR-CON design are described in Table 5. The efficiency of the electric components ranges from 0.95 for the generator to 0.99 for passive components like the cores. The specific power assumed for the components is an average of the recommendation provided by the disciplinary partners. The voltage level is 3000V, which is considered as an advanced technology level but is required to keep the number of parallel conductors for power transmission to a reasonable number.

Table 5 : HDEP components of the SMR-CON obtained for the sizing mission.

Element	Nb	Max power	Efficiency	Specific power	Mass (for 1 el.)	Cooling system
Gas Turbine Generator (or Turboshaft)	2	9.2 MW @ FL 350	0.145 kg/(kW.H)	9 kW (@FL350)/kg	1023 kg	Yes - included in Power density
Generator including AC breakers	4	5.3 MW	0.95	13.5 kW/kg	389 kg	0.5 kg/kW applied to power losses
Converter (AC/ DC) including FCL & DC breakers	4	5.2 MW	0.98	19 kW/kg	273 kg	no
Cables before Core (AWG 3/0)	2 x 8 x 6	3000 V – 303 A max	1	0.817 kg/m +35% for installation and 5% for health monitoring	1506 kg (total mass)	no
Core (or Power Management Unit) including FCL & DC breakers	4	5.1MW	0.99	20 kW/kg	255 kg	no
Cables after Core (AWG 3/0)	2 x 24	3000 V – 303 A max	1	0.817 kg/m +30% for installation and 5% for health monitoring	314 kg (total mass)	no
Inverter (DC / AC) including AC & DC breakers	24	0.835 MW	0.98	19 kW/kg	44.0 kg	no
Electric motor Including fan	24	0.82 MW	0.98	13.2 kW/kg	62.1 kg	no

The following design loop will include a redesign of the REF and BAS aircraft based on a refined fuel consumption evaluation of UHBR turbofans. Similarly, for the SMR-CON, disciplinary work packages will design the main electric components, a thermal management system and a turboshaft based on the current power requirements. These solutions will then be integrated into the OAD tool and the performances of the SMR-CON will be re-evaluated at the end of the next design loop. This work will be part of a future publication.

Structural and aerodynamics analysis are however not the main focus of IMOTHEP for the SMR-CON configuration and no improvements are to be awaited in these disciplines.

4.3 Sensitivities

At the current status of the project, a number of parameters such as TLARs, technology assumptions and system architecture remain subject to uncertainties or could evolve throughout the project. To be more confident in the research path to pursue, a global sensitivity analysis was performed to identify the most influencing variables for the SMR-CON aircraft.

DOI: 10.13009/EUCASS2022-6134

The relative sensitivity of the aircraft performance metrics (such as MTOW, fuel burn,…) with respect to input variables is determined with a variance based approach and the computation of Sobol indices. A short explanation of the Sobol indices is given here.

Figure 6 : aircraft sizing loop representation for calculation of sensitivities.

Considering the aircraft sizing loop with input vector X composed of n variables and the scalar output Y such that $Y = f(X)$, as depicted in Figure 6. The randomness of the input X is assumed to be characterized by a given probability distribution. Thus the output Y is also a random variable with unknown probability distribution. The objective of a variance based sensitivity analysis is to determine which input variable is responsible for the variation of the output.

In order to quantify this ratio, the first-order Sobol indices are a measure of the variation of Y with the variability of X_i, normalized by the total variation of Y. They are defined by [9]:

$$S_i = \frac{Var(E[Y|X_i])}{Var(Y)},$$

where $E[Y|X_i]$ is the conditional expected value of Y when X_i is fixed and the other variables $X_{j\neq i}$ are varying. $Var(E[Y|X_i])$ is the variance over the domain of definition of X_i.

Considering as simple example a process governed by the function $f(x_1, x_2) = 2x_1 + 5$, this function depends only on x_1. Given two random variables X_1 and X_2, one can compute the conditional expected values $E(Y|X_1)$ and $E(Y|X_2)$ as presented in Table 6.

Table 6: Expected mean value and variance for a simple function

$Y = 2X_1 + 5$		X_1			
		1	-1	3	$E(Y\|X_2)$
X_2	-1	7	3	11	7
	2	7	3	11	7
	-2	7	3	11	7
$E(Y\|X_1)$		7	3	11	
$Var(E(Y\|X_1))$		17			
$Var(E(Y\|X_2))$		0			

In this short example, Y takes only three values [7, 3, 11] and $Var(Y) = 17$. Therefore the Sobol indices are $S_1 = 1$, the variance $Var(Y)$ is entirely explained by the variation of variable X_1 and inversely with $S_2 = 0$, the variation of variable X_2 does not influence the output.

Different methodologies are available to compute the Sobol indices. To limit the number of function evaluations and to treat discrete input variables, a sparse Polynomial Chaos Expansion method is employed [10].

In such a preliminary phase, this analysis is useful to understand the relative influence of the uncertain variables on the aircraft design performances. The distribution of the propulsive components allows a better sizing (through reduced oversizing). Hence, it may be interesting to have a heavily distributed architecture. At the same time, electric machines have varying specifications depending on the size, torque and rotation speed they have to achieve, which depend on the selected architecture and distribution. The problem can be tackle from one side or the other and in an attempt to give a priority, the sensitivity analysis will focus on the effects that electric machines characteristics and architecture distribution have on the aircraft performances.

DOI: 10.13009/EUCASS2022-6134

A design of experiments consisting of 170 points sampled via Latin Hypercube Sampling technic [11], was created assuming uniform distribution of the input within the bounds given in *Table 7*.

Table 7 : Variables considered for calculated the Sobol indices

Variables	Type	Field	Field	Field	Field	Field
Emotor number	Discrete	8	16	24	32	40
Core number	Discrete	2	4	6	8	
Generator per turbomachine	Discrete	1	2	3	4	
Turbomachine number	Discrete	2	3	4	5	6
	Type	Min	Max			
Specific power of electric machines	Continuous	10	17			
Efficiency of electric machines	Continuous	0.95	0.98			

It is important to note that at this point of the study, the variables used for the DoE are considered independent while in reality they are not and some combinations are not possible. The interdependencies are simply not modelled in the OAD sizing code, so freedom is taken with the design knowing that the variable dependencies will be brought by disciplinary specialists to isolate feasible designs during post-processing. The selected design will then be baselines for all partners to start working on disciplinary solutions.

Table 8: First order Sobol Indices

	MTOW		Mission fuel	
Variables	First order Sobol index	Variation (%) over 100 repetition	First order Sobol index	Variation (%) over 100 repetition
Fan number	1.65E-02	30.8	2.09E-02	16.9
Core number	2.00E-02	35.5	7.72E-03	24.7
Generator per turbomachine	2.32E-03	156.0	1.37E-03	89.3
Turboshaft number	**2.87E-01**	7.4	**4.70E-01**	3.5
E-machine specific power	**3.71E-01**	6.3	**1.39E-01**	5.8
E-machine efficiency	**2.16E-01**	10.6	**3.30E-01**	4.5
First order sum	9.13E-01		9.70E-01	

The sobol indices for the MTOW and fuel burn are presented in Table 8. Associated are the 2D plots in Figure 7. The MTOW and the fuel burn do not show a sensitivity to fan number, core number or generator per turbomachine. The sizing rules of the architecture, although ensuring less oversizing for higher distribution are not influencing the performances compared to the variation of electric machine efficiency and specific weight or turboshaft number. On the contrary, this last variable has a large influence due to the worst thermal efficiency of small turbomachine and the added wetted surface area. This is visible in the 2 plots were the large dispersion of the MTOW and fuel burn as function of the fan number does not allow to observe a dependency, contrary to the plot as function of the turboshaft number.

Although the MTOW shows a high dependency on the specific weight of electric machines, the fuel burn is most sensitive to the variation of the electric machines efficiency. This shows the direction of research to improve the design. If weight is the primary performance to improve, then efforts should be put into a better estimation of the achievable specific weight of the electric machine. Inversely, if the fuel burn is the most important metric, efforts should primarily be put into a better estimation of electric machine efficiency. Furthermore, considering the range of variations given at this step, the focus should be on improving components characteristics, the distribution inducing only small changes in comparison.

DOI: 10.13009/EUCASS2022-6134

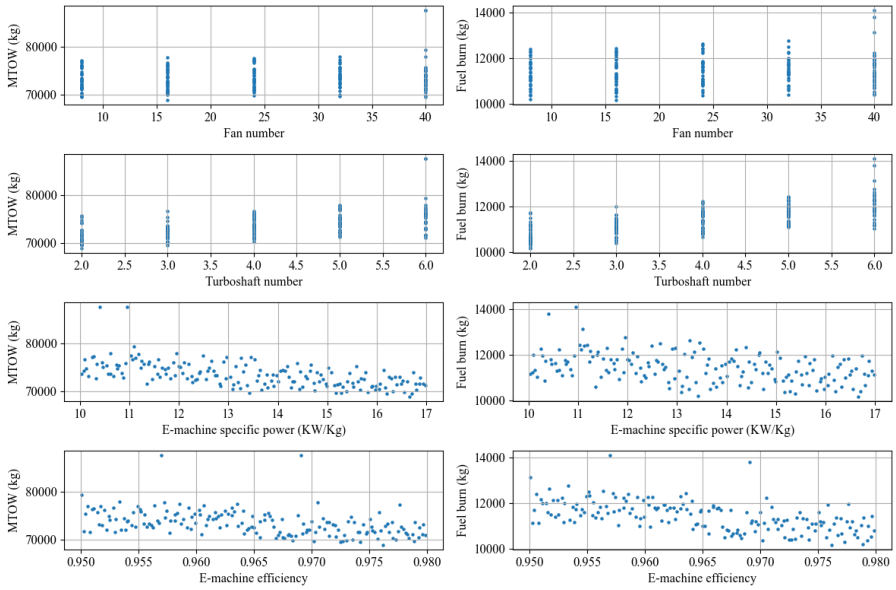

Figure 7: two-dimensional plots of the DOE used for the calculation of the SOBOL indices.

5.0 EPU detailed modelling

The perimeter of the Electrical Propulsion Unit (EPU) is defined from the electrical network connection to the shaft driving a propeller or a fan (see Figure 8). From the previous analysis, new needs appear on the design of EPU as well as on the architecture of the electrical components involved in this system.

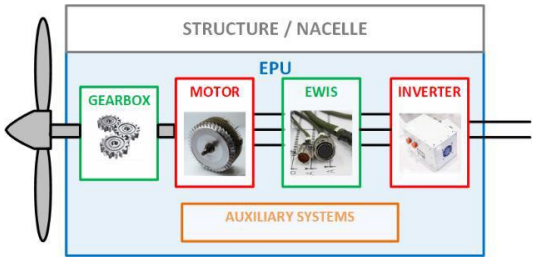

Figure 8: Illustration of the EPU perimeter

This section focuses on one hand on the preliminary design of the electrical machine dedicated to the EPU and on other hand on EPU preliminary architecture.

5.1 Electrical Machine preliminary design

For the SMR-CON concept, appropriate high power density electrical machines are sized, using an in-house developed Genetic-Algorithm (GA)-based multi-domain electrical machine sizing tool [12]. The SMR-CON concept presents an interesting challenge for the motor, which differently to many existing high kW/kg propulsion machines requires a comparatively smaller outer diameter and a higher length. The machines are sized for different cooling concepts and various thermal limits corresponding to different insulation recipes.
The machine specifications are as follows :

- Power = 820kW
- RPM = 5700 rpm
- Motor outer diameter ≤ 220mm
- Length of the machine ≤ 780mm
- Frequency ≤ 1kHz;
- Topology : Halbach surface-PM

DOI: 10.13009/EUCASS2022-6134

• Core Material : Thin Cobalt-Iron alloy

The machines are sized as shown in *Figure 9*, in seeking the best kW/kg under the thermal constraints. Some parameters, such as thermal properties, including thermal conductivity, are set as constant values, together with the machine constraint parameters, including power, speed, rpm, DC link voltage, and material specific parameters. Machine geometrical parameters are set as variables, which are determined in the optimization process. These include geometrical variables such as, magnet thickness, form factor, split ratio, tooth width and tooth height coefficient from electromagnetic and thermal parameters depending on different cooling techniques. Constraint parameters include the thermal limit, i.e, the peak temperature in the electrical machine.

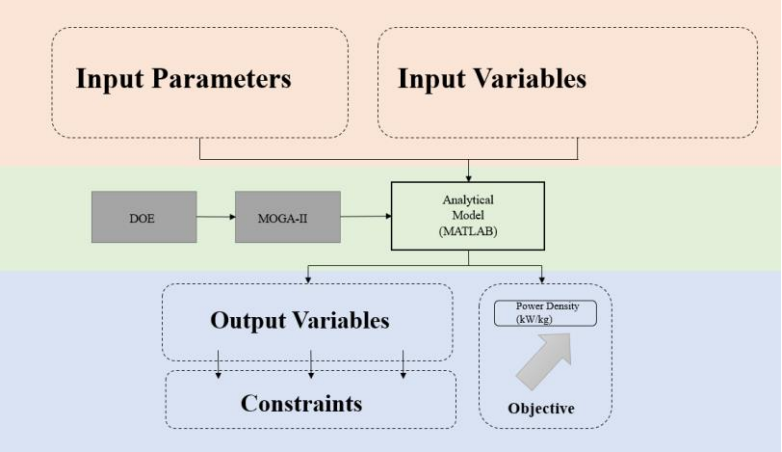

Figure 9: Multi-domain optimization process

The cooling techniques considered include using oil and air as coolants. Enhanced oil cooling method is as shown in *Figure 10*, where basically the coolant oil is in direct contact with the winding. A semi-flooded oil-cooling concept is used whereby a stator sleeve separates the machine in a wet-region (stator) and a dry region (rotor), thus helping dissipate the high losses in the coil, without causing excessive windage losses in the rotor. Slot cooling channels are created for the oil to flow through, further enhancing the heat dissipation as described in [13], [14].

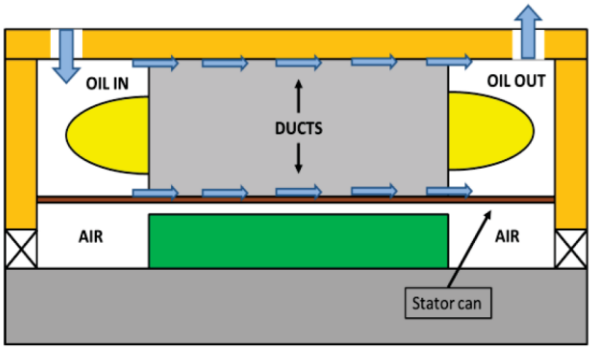

Figure 10: Semi-flooded oil cooling [12]

Two types of air-cooling techniques are investigated and compared for the SMR-CON machine: (i) conventional external air cooling, and (ii) advanced air cooling.

For the conventional air forced cooling, the external air blows over the finned machine as shown in *Figure 11*, while with the advanced air-cooling concept involves the air ventilation cooling inside the machine and directly removes the heat generated within the machine.

DOI: 10.13009/EUCASS2022-6134

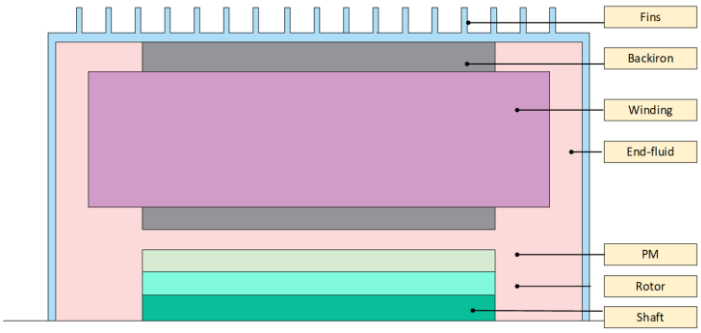

Figure 11: external air cooling.

Table 9: Achievable power densities for investigated cooling concepts under different temperature limits.

	Parameter	Unit	180°C thermal limit	220°C thermal limit	300°C thermal limit
External air cooling	Peak temperature	°C	186.57	222.37	306.31
	Current density	A/mm^2	4.1	5.2	6.6
	Power density	kW/kg	1.8	2.4	3.1
Advanced air cooling	Peak temperature	°C	179.11	222.44	302.33
	Current density	A/mm^2	10.1	12.6	14.5
	Power density	kW/kg	6.1	7.3	8.5
Oil cooling	Peak temperature	°C	182.42	218.57	301.03
	Current density	A/mm^2	21.06	25.81	30.93
	Power density	kW/kg	12.9	14.8	16.6

The achievable power densities for the 820kW 5700rpm machine for the investigated thermal management techniques under different temperature limits are summarised in Table I. From the calculation reaching 10kW/kg with oil is a realistic prospect. On the other hand external air-cooling is quite limited in achieving the target high gravimetric power density. The main bottleneck with external cooling is the high thermal resistance path for the copper losses due to the equivalent slot thermal conductivity. While the conductivity of copper is high, in reality the slot contains multiple materials (impregnation, slot liner, enamel, air-bubbles etc.) which have low thermal conductivity. A way to improve the situation with air cooling is to force air into the machine. Using such advanced air cooling concept, while the target power density is still not met, it is approached, and through further in-depth optimisations might be met.

5.2 EPU architectural considerations

A detailed system architecture analysis allowed highlighting the main functions of the EPU in a generic approach [15]. Based on this analysis, some specific investigations have been done on the two main topics linked to the SMR-CON targets in terms of specific power and cooling strategy. The two architecture options are:

- **Direct Drive (DD) versus Integral Drive (ID)**:

In a direct drive option, the rotational speed of the EPU is equal to the one of the fan or propeller. Some applications require direct drive interface due to specific operating points (as high torque at low speed) and the electrical machine is designed to address the requirement and tends generally to an" annular" shape factor (length to diameter ratio).

DOI: 10.13009/EUCASS2022-6134

In the integrated drive, there is different rotational speeds between the electrical machine and the propulsive device by the use of a gearbox. In this way, the electrical machine can be designed with higher rotational speed allowing an increase in specific power for the same mechanical power. A first investigation is presented hereafter on the assessment of the specific power of such architectures.

- **Air-cooled option with an integrated power electronics**:

In an integrated option, the power electronic is close to the electrical machine, and both components are packaged in a same equipment, limiting the interfaces and the use of dV/dt filter. This option allows optimizing the overall system and airframe integration (one LRU to manage), and limiting auxiliary interfaces (sensors, mutualisation of cooling management…). The weight is reduced by the elimination of cables, the absence of filter on AC side and a better optimisation between the electrical machine and the power electronics.

With a power level of about 800 kW, air-cooling for the electrical machine and the power electronics (PE) is a challenge. The difficulty is further increased as the key design driver for the optimisation is related to the total weight of the EPU. Nevertheless, considering some hypothesis on the air-cooling technology and parameter, a first analysis has been done to evaluate the feasibility of this architecture. To this end, an integrated PE is considered in the architecture.

Based on a preliminary design of the EPU and dedicated electrical machine, sensitivity analysis have been done by varying the design rotational speed of the electrical machine in order to carry out a trade-off between Direct Drive (DD) and Integral Drive (ID) architectures. The preliminary design of the gearbox for the ID architecture is the result of internal tools taking into account state of the art aeronautics gearbox designs and ensuring compliance with the constraint envelope of the electrical machine. There is no optimisation in this first step regarding the mutualisation of structure (housing), cooling, accessories and on the overall integration. Only the combination of two separate designs: electrical machine and gearbox, is performed.

The sensitivity analysis was made with the following hypothesis:

- GearBox (GB): Design based on epicyclical architecture. Integer gearbox ratio. Active parts (gears, bearing, carrier) and passive parts (structures and housing) are included.
- Electrical machine: Design based on PMSM topology. Active and passive parts are included. Limits on winding temperature (180°C) and rotor tip speed (200 m/s).
- Two cooling options have been considered: forced air cooled and liquid cooling for comparison.

The results for the EM preliminary sizing relating specific weight to the rotational speed are illustrated in Figure 12.

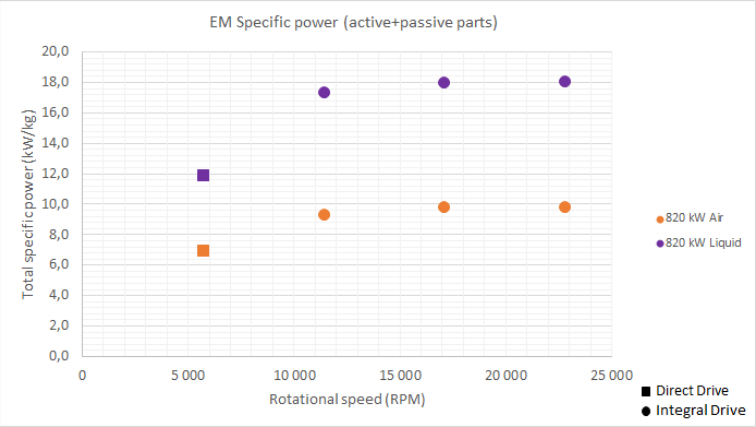

Figure 12: Electrical machine design for DD and ID architecture comparison for SMR-CON

The results for DD and ID architectures are depicted on Figure 13 and Figure 14.

DOI: 10.13009/EUCASS2022-6134

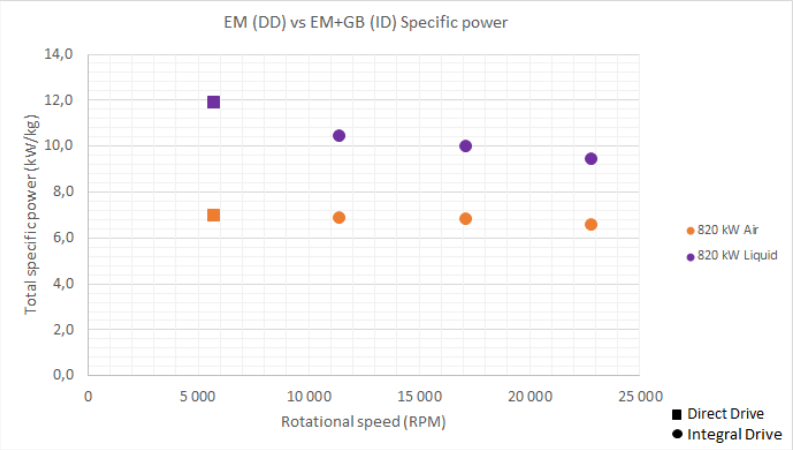

Figure 13: Direct Drive (DD) and Integral Drive (ID) specific power for the EPU architecture including EM and PE for the SMR-CON

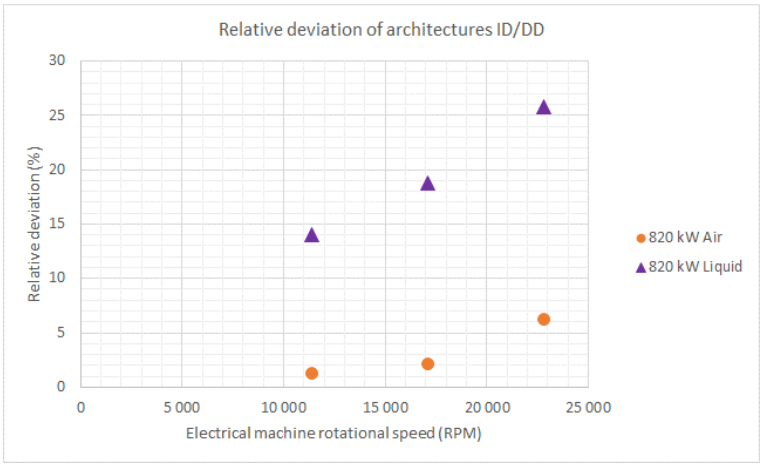

Figure 14: Relative difference between the Direct Drive design and the three ID design.

Due to the limited volume dedicated to the electrical machine, especially the small outer diameter of 260 mm, and to the initial rotational speed of the DD architecture, 5 700 RPM which is high for a propeller but envisioned for fan, the integral drive architecture has no gain in term of weight and so in specific power. On the contrary, the weight can increase up to 25% compared to the DD architecture with liquid cooling. The air cooled option seems to be less sensitive but with the challenge to manage efficiently the temperature of both the electrical machine (with the power electronics) and the gearbox.

A second investigation has been carried out on the capability to define an integrated power electronics with the electrical machine using a common air-cooled architecture.
In order to validate or improve this assumption, a preliminary study has been carried out in parallel of the design of Electrical Machine and Power Electronics by the use of thermal numerical simulation (Finite Element Method).
This study considers a unique heat sink for the electrical machine and the power electronics, following an integrated drive architecture. To enhance the heat transfer capability, staggered fins are added on the outer diameter of the heat sink yoke as illustrated in Figure 15. The heat sink is made of aluminium material.

DOI: 10.13009/EUCASS2022-6134

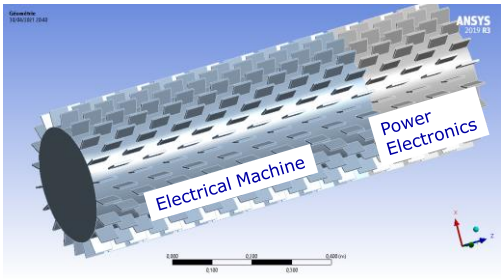

Figure 15: Numerical model of the heat sink for integrated drive EPU

Sensitivity analysis are performed on the total number of fins (20 or 60), on the fin length (5, 10 or 20 cm) and on the heat transfer coefficient (50 to 300 W/m2.K) to represent forced air convection. Note that the convection coefficient is homogeneous over the entire surface of the heat sink.
The losses are imposed in the inner surface of the heat sink yoke, at the interface with the electrical machine and the power electronics with references and values depicted in the Table 10.

Table 10: Input parameter for the numerical simulations

Continuous Power [kW]	820	845
Efficiency [%]	97.0	98.8
Length [mm]	800	300
Heat flux [kW/m2]	38.8	41.0

Figure 16 and Figure 17 illustrate the results of the numerical simulations reporting the maximum temperature in steady state at the inner surface of the heat sink considering a 25°C ambient temperature.
Logically, the difference in temperature between the PE and the EM is low because they share the same heatsink yoke. For the height of the fins, an asymptote is quickly reached around 10 cm, which is already a large dimension.

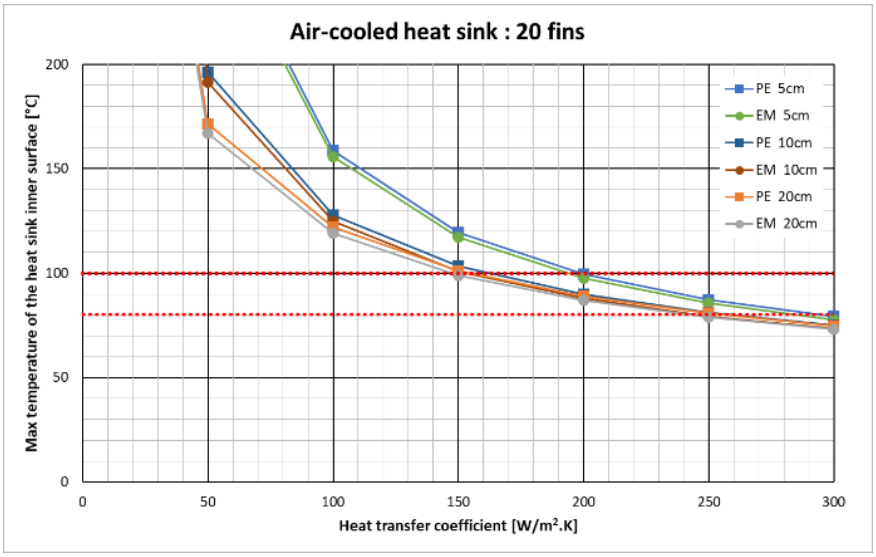

Figure 16: Numerical simulation results, maximum temperature of the heat sink inner surface with 20 fins

DOI: 10.13009/EUCASS2022-6134

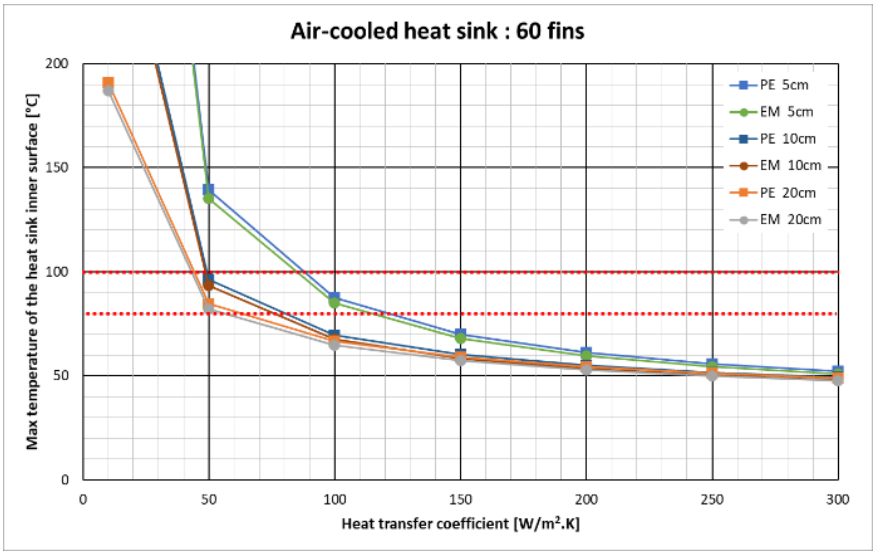

Figure 17: Numerical simulation results, maximum temperature of the heat sink inner surface with 60 fins.

Thus, it is possible to determine the range of heat transfer coefficient allowing reaching the base plate temperature of the power module and to define the technology able to generate and control these heat flows. The values are summarized in Table 11. For further analysis, this work has to be interpreted in temperature difference with respect to other ambient temperature and environment.

Table 11: Synthesis of the Heat Transfer Coefficient (HTC) to ensure base plate temperature of the power module between 80°C and 100°C

Number of fin	20 fins		60 fins	
Fin height [mm]	50	100	50	100
HTC min [W/m^2.K]	200	150	90	50
HTC max [W/m^2.K]	300	250	120	80

Note that the power electronics imposes the maximum inner surface temperature. The electrical machine supports higher temperature (close to 150°C) at the outer surface of the stator.

This analysis has to be consolidated by deeper investigations related to the propeller design concerning the following points at least:

- The losses were allocated homogenously on the inner surface of the heat sink. What is the impact on the power module if the losses are located in a defined area (concentration of the heat flux)?
- The heat transfer coefficient is homogeneous on the external surface of the heat sink. More accurate simulations like 3D CFD have to be planned in order to define a more precise air flow behaviour (taking into account turbulence) and the increase in air temperature along the length of the heat sink (gradient of the “cold” air at the surface of the heat sink).
- Transpose the HTC parameter in duct geometry and flow rate to estimate the capability to use the ducted fan airflow (during all flight phases, especially on ground) or to define the requirement for a dedicated cooling channel.
- Consolidate the geometry and the design of the heat sink to optimise the integration, efficiency and weight at the EPU level.
- And finally, what are the consequences on the aircraft drag of such air-cooled devices and heat sink topology considering the high number of e-Fan (24 for all the aircraft).

6.0 Conclusion

The architecture and the sizing procedure of a full turboelectric distributed propulsion aircraft was presented. It was shown that each propulsive component may be sized by a different flight condition and that the requirements of the standard mission are more demanding than failure scenario in terms of maximal rated power. The intrinsically high redundancy of the propulsive architecture allowing to limit the impact of one component failure.

DOI: 10.13009/EUCASS2022-6134

The SMR-CON aircraft, despite a higher empty weight and a lower lift to drag ratio, shows a fuel burn 6.5% lower than the reference 2035 high by-pass ratio turbofan aircraft. The improved propulsive efficiency offered by distribution of the propulsion balances the increased weight and reduced lift to drag ratio. It was also shown that within the work planned in the IMOTHEP project, the most effective way to further improve the confidence in the performances of the SMR-CON is to increase the accuracy in the prediction of electric components characteristics (efficiency and specific weight) before optimizing the propulsive architecture.

Following this result, the preliminary design of the EPU based on the power requirements deduced from the first OAD design loop was presented. An integrated EPU architecture is selected considering the advantage it brings on a system point of view. Additionally in the case of the SMR-CON, a Direct Drive EPU was found to be the most advantageous to reach high specific weight. Finally, liquid and air cooling options are analysed and the corresponding performances of the EPU are given.

In the next design loops, the SMR-CON aircraft will beneficiate from new component designs provided by IMOTHEP partners, this includes: turboshaft; electric motor and power electronics; generators and thermal management system.

Funding: This project has received funding from the European Union's Horizon 2020 research and innovation program under grant agreement No 875006 IMOTHEP

References

[1] A. H. Epstein, « Aeropropulsion for Commercial Aviation in the Twenty-First Century and Research Directions Needed », *AIAA Journal*, vol. 52, nº 5, p. 901-911, mai 2014, doi: 10.2514/1.J052713.

[2] P. Schmollgruber *et al.*, « Multidisciplinary Exploration of DRAGON: an ONERA Hybrid Electric Distributed Propulsion Concept », présenté à AIAA Scitech 2019 Forum, San Diego, California, janv. 2019. doi: 10.2514/6.2019-1585.

[3] P. Schmollgruber *et al.*, « Multidisciplinary Design and performance of the ONERA Hybrid Electric Distributed Propulsion concept (DRAGON) », présenté à AIAA Scitech 2020 Forum, Orlando, FL, janv. 2020. doi: 10.2514/6.2020-0501.

[4] P. Schmollgruber, N. Bartoli, J. Bedouet, S. Defoort, Y. Gourinat, et E. Bénard, « Use of a Certification Constraints Module for Aircraft Design Activities », Denver, United States, 2017. [En ligne]. Disponible sur: https://hal.archives-ouvertes.fr/hal-02045709

[5] C. David, S. Delbecq, S. Defoort, P. Schmollgruber, E. Benard, et V. Pommier-Budinger, « From FAST to FAST-OAD: An open source framework for rapid Overall Aircraft Design », *IOP Conf. Ser.: Mater. Sci. Eng.*, vol. 1024, p. 012062, janv. 2021, doi: 10.1088/1757-899X/1024/1/012062.

[6] S. Defoort *et al.*, « Conceptual design of disruptive aircraft configurations based on High-Fidelity OAD process », in *2018 Aviation Technology, Integration, and Operations Conference*, American Institute of Aeronautics and Astronautics, 2018. doi: 10.2514/6.2018-3663.

[7] « Devis de masse des avions, AIR 2001/D », DGA - Direction Générale de l'Armement, Norme AIR 2001/D, 1984.

[8] J. Hermetz, M. Ridel, et C. Doll, « Distributed electric propulsion for small business aircraft a concept-plane for key-technologies investigations. », DAEJEON, South Korea, 2016, p. 11.

[9] I. M. Sobol', « On sensitivity estimation for nonlinear mathematical models », *Matematicheskoe modelirovanie*, vol. 2, nº 1, p. 112-118, 1990.

[10] G. Blatman et B. Sudret, « Adaptive sparse polynomial chaos expansion based on least angle regression », *Journal of Computational Physics*, vol. 230, nº 6, p. 2345-2367, mars 2011, doi: 10.1016/j.jcp.2010.12.021.

[11] J. Sacks, W. J. Welch, T. J. Mitchell, et H. P. Wynn, « Design and analysis of computer experiments », *Statistical science*, vol. 4, nº 4, p. 409-423, 1989.

[12] D. Golovanov, L. Papini, D. Gerada, Z. Xu, et C. Gerada, « Multidomain Optimization of High-Power-Density PM Electrical Machines for System Architecture Selection », *IEEE Transactions on Industrial Electronics*, vol. 65, nº 7, p. 5302-5312, 2018, doi: 10.1109/TIE.2017.2772188.

[13] Z. Xu *et al.*, « A semi-flooded cooling for a high speed machine: Concept, design and practice of an oil sleeve », in *IECON 2017 - 43rd Annual Conference of the IEEE Industrial Electronics Society*, 2017, p. 8557-8562. doi: 10.1109/IECON.2017.8217503.

[14] D. Golovanov *et al.*, « 4-MW Class High-Power-Density Generator for Future Hybrid-Electric Aircraft », *IEEE Transactions on Transportation Electrification*, vol. 7, nº 4, p. 2952-2964, 2021, doi: 10.1109/TTE.2021.3068928.

[15] C. Maury, C. Viguier and Y. Fefermann, "Design and architectures of hybrid/all Electrical Aircraft", MEA 2021, Bordeaux, France, 20-21 October 2021.